



Contents lists available at ScienceDirect

Biochemical and Biophysical Research Communications

journal homepage: www.elsevier.com/locate/ybbrc

Moyamoya disease patient mutations in the RING domain of RNF213 reduce its ubiquitin ligase activity and enhance NFκB activation and apoptosis in an AAA+ domain-dependent manner

Midori Takeda ^{a,b}, Tohru Tezuka ^{a,c,*}, Minsoo Kim ^d, Jungmi Choi ^{a,b}, Yuki Oichi ^{a,e},
Hatasu Kobayashi ^f, Kouji H. Harada ^b, Tsunehiro Mizushima ^g, Shigeru Taketani ^a,
Akio Koizumi ^{b,h}, Shohab Youssefian ^a

^a Laboratory of Molecular Biosciences, Graduate School of Medicine, Kyoto University, Kyoto, Japan

^b Department of Health and Environmental Sciences, Graduate School of Medicine, Kyoto University, Kyoto, Japan

^c Human Biosciences Unit for the Top Global Course, Center for the Promotion of Interdisciplinary Education and Research, Kyoto University, Kyoto, Japan

^d The Hakubi Center for Advanced Research, Kyoto University, Kyoto, Japan

^e Department of Neurosurgery, Graduate School of Medicine, Kyoto University, Kyoto, Japan

^f Department of Environmental and Molecular Medicine, Graduate School of Medicine, Mie University, Mie, Japan

^g Graduate School of Life Science, University of Hyogo, Hyogo, Japan

^h Institute of Public Health and Welfare Research, Kyoto, Japan

ARTICLE INFO

Article history:

Received 19 January 2020

Accepted 4 February 2020

Available online xxx

Keywords:

Moyamoya disease

RNF213

Ubiquitin ligase

Ubiquitination

NFκB

Apoptosis

ABSTRACT

Moyamoya disease (MMD) is a cerebrovascular disease characterized by progressive occlusion of the internal carotid arteries. Genetic studies originally identified RNF213 as an MMD susceptibility gene that encodes a large 591 kDa protein with a functional RING domain and dual AAA+ ATPase domains. As the functions of RNF213 and its relationship to MMD onset are unknown, we set out to characterize the ubiquitin ligase activity of RNF213, and the effects of MMD patient mutations on these activities and on other cellular processes. *In vitro* ubiquitination assays, using the RNF213 RING domain, identified Ubc13/Uev1A as a key ubiquitin conjugating enzyme that together generate K63-linked polyubiquitin chains. However, nearly all MMD patient mutations in the RING domain greatly reduced this activity. When full-length proteins were overexpressed in HEK293T cells, patient mutations that abolished the ubiquitin ligase activities conversely enhanced nuclear factor κB (NFκB) activation and induced apoptosis accompanied with Caspase-3 activation. These induced activities were dependent on the RNF213 AAA+ domain. Our results suggest that the NFκB- and apoptosis-inducing functions of RNF213 may be negatively regulated by its ubiquitin ligase activity and that disruption of this regulation could contribute towards MMD onset.

© 2020 The Authors. Published by Elsevier Inc. This is an open access article under the CC BY-NC-ND license (<http://creativecommons.org/licenses/by-nc-nd/4.0/>).

1. Introduction

Moyamoya disease (MMD) is a rare idiopathic cerebrovascular disorder characterized by occlusive lesions at the terminal portion of the internal carotid arteries. The gene encoding the Ring finger protein 213 (RNF213) was previously identified as the major susceptibility gene for MMD in East Asian populations by genome-wide linkage analysis and exome analysis [1,2]. Since then, more

than 50 mutations have been identified in RNF213 [3,4], with the coding variant p.R4810K being strongly associated with MMD in the Japanese and Korean and, to a lesser extent, in the Chinese population [1,3]. Recently, p.R4810K has been identified as a risk allele for other vascular occlusive diseases, including pulmonary arterial hypertension [5] and large-artery atherosclerosis [6], suggesting that dysregulation of RNF213 functions may lead to a wide variety of vasculopathies.

Previous studies have reported that RNF213 is involved in various cellular functions, including cell cycle progression and lipid responses [7–9]. However, the molecular mechanisms by which RNF213 mutations modify these cellular functions and lead to the

* Corresponding author. Laboratory of Molecular Biosciences, Graduate School of Medicine, Kyoto University, Kyoto, Japan.

E-mail address: tezuka.toru.8w@kyoto-u.ac.jp (T. Tezuka).

<https://doi.org/10.1016/j.bbrc.2020.02.024>

0006-291X/© 2020 The Authors. Published by Elsevier Inc. This is an open access article under the CC BY-NC-ND license (<http://creativecommons.org/licenses/by-nc-nd/4.0/>).

various vasculopathies remain unresolved. RNF213 is a huge protein of 591 kDa containing two functional domains; dual AAA+ ATPase domains and a RING domain [1]. Its two AAA+ domains are important for oligomerization and presumably subsequent activation [10], whereas the RING domain possesses ubiquitin ligase activity [1]. The ubiquitination of target proteins requires three types of enzymes; ubiquitin (Ub) activating enzyme (E1), Ub conjugating enzyme (E2), and a ubiquitin ligase (E3) that binds to and determines the substrates to be ubiquitinated. Ubiquitination is a cascade reaction that conjugates Ub to substrate proteins, followed by additional conjugation of Ub through one or more of its seven lysine residues [11]. The fate of polyubiquitinated substrates depends on the Ub linkage type, which is generally related to the specific E2 [11,12]. K48-linked polyubiquitin chains target substrates for proteasomal degradation, whereas K63-linked chains exert non-degradative roles in intracellular trafficking, inflammatory signaling, and other processes [13]. However, E2(s) that cooperate with RNF213 have not been studied, and the physiological or pathophysiological functions as well as the underlying mechanisms of RNF213-mediated ubiquitination remain unresolved.

Thus, in this study, we investigated the biochemical characteristics of the RNF213 RING domain, and examined the effects of MMD patient RING mutations on E3 activity and on several induced cellular processes, as well as the importance of its AAA+ domains on these processes.

2. Materials and methods

2.1. Cell culture and transfection

Human embryonic kidney 293T (HEK293T) cells were cultured in Dulbecco's modified Eagle's medium (Nacalai Tesque) containing 10% fetal bovine serum (Thermo Fisher) and 100 units/ml penicillin (Nacalai). Cells were transfected with Viofectin (Viogene) according to the manufacturer's protocol.

2.2. Antibodies and reagents

Primary and secondary antibodies used in this study are listed in [Supplementary Table 1](#). Wild-type (WT) Ub protein for *in vitro* ubiquitination assays (except that used in [Fig. 1C](#)), Cycloheximide (CHX), and Quinazoline (QNZ) were from Merck; Adenosine 5'-triphosphate (ATP) from Oriental Yeast; Quick Coomassie Brilliant Blue (CBB) was from Wako.

2.3. DNA constructs

Details of DNA constructs used in this study are described in [Supplementary Methods](#). Bacterial expression plasmids of E2s except for E2-25K, Ube2G2 and UbcH10 were as described [14,15]. Mammalian expression plasmids pcDNA-3×FLAG-RNF213 (WT and D4013N) were as described [16].

2.4. Protein purification

His-E1 was purified as described [15]. His-Ubc13 was expressed in BL21(DE3) *E. coli* cells and purified using Ni-NTA Superflow beads (QIAGEN). GST-E2 proteins were expressed in BL21(DE3), purified by glutathione–Sepharose 4B, and the GST removed with PreScission™ protease (GE Healthcare). Untagged ubiquitin WT or K mutants were purified by cation exchange chromatography [Hi/Trap (SP); GE Healthcare] [17]. AMSH was purified as described [18]. GST-RNF213RING was expressed in BL21(DE3), purified by glutathione–Sepharose 4B, and eluted with glutathione. Purified

proteins were dialyzed against dialysis buffer (20 mM Tris pH 7.5 and 1 mM DTT), verified by CBB staining, and quantified using Protein Assay CBB (Nacalai) with an Infinite 200 PRO reader (TECAN).

2.5. *In vitro* ubiquitination assays

E3 enzymes [GST-RNF213RING, WT or mutants (final 87.5 ng/μL)] were mixed with Ub [WT or mutants (6.25 ng/μL)], E1 (3 ng/μL) and E2 [Uev1A (15 ng/μL), others (8 ng/μL)] in ubiquitination buffer (50 mM Tris pH 7.5, 5 mM MgCl₂, 2 mM DTT and 0.4 mM ATP) in 40 μL volume. Reaction mixtures were incubated at 30 °C for 60 min, stopped by SDS sample buffer, and subjected to immunoblotting. In the deubiquitination experiments, reactions were incubated at 30 °C for 4 h with 5 mM ATP, stopped by addition of 1 mM EDTA, pulled-down with glutathione–Sepharose 4B, and finally washed with ubiquitination buffer. AMSH (7.5 ng/μL) was added to the mixture and incubated at 30 °C for 30 min.

2.6. Immunoblotting

Ubiquitination reaction mixtures or cell lysates were separated in 5–20% SDS-PAGE gels (Nacalai), transferred onto PVDF membranes (Merck), with blocking, incubation with primary and secondary antibodies and appropriate washing basically as described [19]. Chemiluminescent signals were developed by ECL Prime (GE Healthcare) or CDP-star (NEB), and analyzed using a LAS3000 imager and Multi Gauge software (GE Healthcare).

2.7. NFκB dual luciferase assays

HEK293T cells were transfected with various combinations of the following plasmids: firefly luciferase expression plasmid driven by NFκB-responsive elements (pGL4.32, Promega), Renilla luciferase expression plasmid driven by the HSV thymidine kinase promoter (pGL4.74) as an expression control, and pcDNA3.1 empty vector or 3×FLAG-RNF213 expression plasmid at a final ratio of 1:0.1:3. Cells were lysed 40 h post-transfection and subjected to dual-luciferase reporter assays (Promega) using a multi-label plate reader ARVO X5 (PerkinElmer).

2.8. CHX chase assays

HEK293T cells were transfected with pcDNA-3×FLAG-RNF213 (WT or mutants) and treated with CHX (20 μg/ml) 24 h post-transfection. At indicated time points, cells were lysed in TNE buffer (50 mM Tris-HCl pH 8.0, 150 mM NaCl, 2 mM EDTA, 1% NP-40) with a Protease Inhibitor Cocktail (Nacalai).

2.9. Apoptosis assays

HEK293T cells were transfected with pcDNA-3×FLAG-RNF213 (WT or mutants)-IRES-enhanced green fluorescent protein (EGFP) or a control EGFP expression plasmid. Cells were harvested 40 h post-transfection, labelled with APC Annexin V and propidium iodide (PI) (BioLegend), and subjected to flow cytometry. Data were collected and analyzed using FACS Aria II with FlowJo software (BD Biosciences). In the QNZ experiments, QNZ (30 nM) was added 20 h post-transfection.

2.10. Structural modeling

Homology models of the RNF213 RING domain (residues 3994–4057) were generated using Swiss-Model server [20] on the basis of the RING domain structure of RNF8 (Protein Data Bank ID

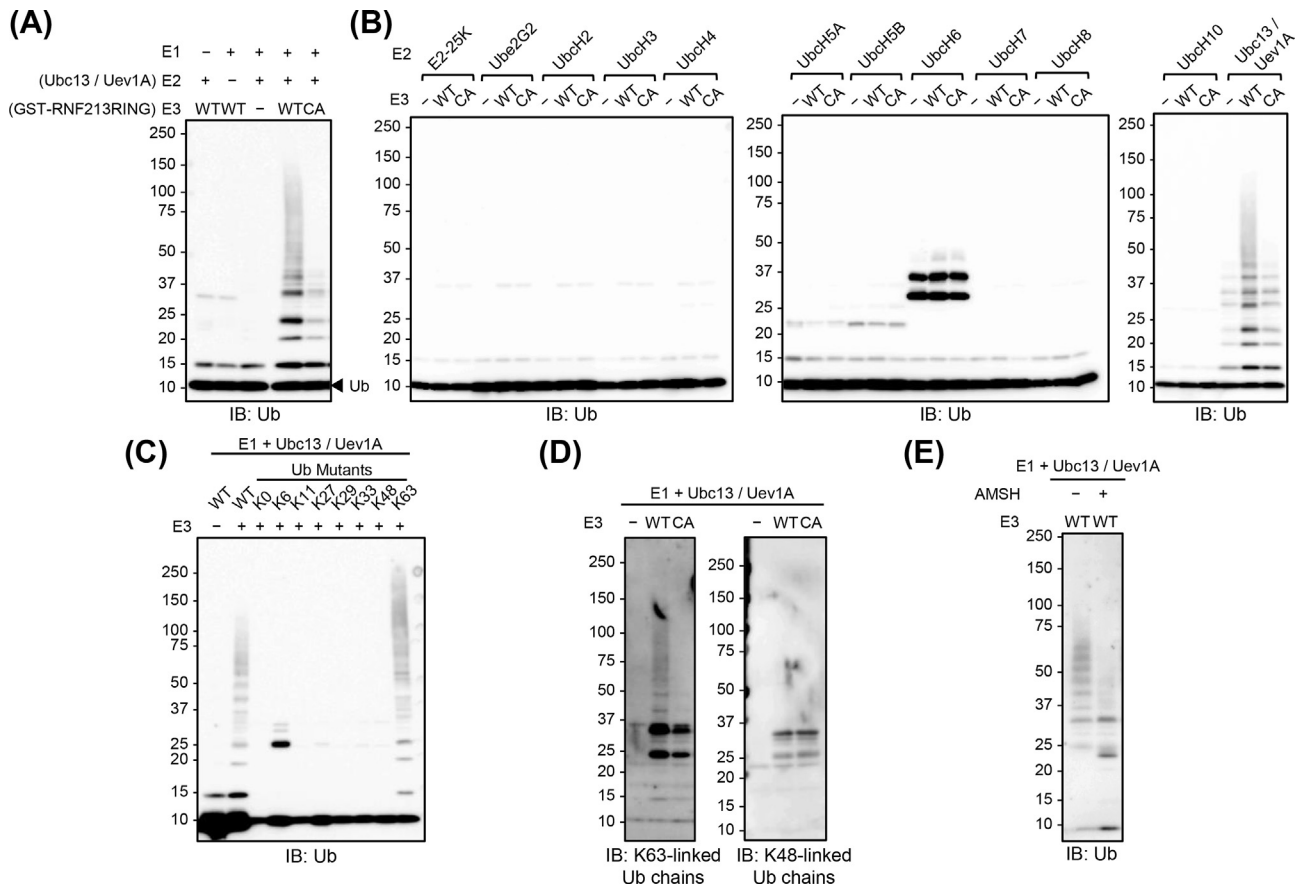


Fig. 1. RNF213 RING domain selectively cooperates with Ubc13/Uev1A to generate K63-linked polyubiquitin chains *in vitro*.

(A–E) *In vitro* ubiquitination reactions performed using a GST-RNF213 RING domain fusion protein as E3 with various E1 and E2 combinations. Reaction products were immunoblotted (IB) with antibodies against Ub (A–C, E), and K63-, or K48-linked polyubiquitin (D). (A and D) Reactions with indicated E1, E2 (Ubc13/Uev1A), and E3 combinations. (B) Reactions with various E2s. (C) Reactions with various WT and mutant Ub. (E) Reaction mixtures treated with or without AMSH, a K63 linkage-specific deubiquitinase. WT, wild-type. CA, C3997A E3-dead mutant. (–), absence.

code 4ORH) as template. The RNF213 RING dimer–Ubc13 complex model was simply constructed by superposition of the RING subunits from RNF213 RING and RNF8 dimer–Ubc13 structures (PDB ID code 4ORH).

2.11. Data analysis

Statistical significance was evaluated by one-way ANOVA with Tukey–Kramer multiple comparisons test using InStat software (GraphPad). $p < 0.05$ indicates statistical significance.

3. Results

3.1. RING domain of RNF213 coupled with Ubc13-Uev1A generates K63-linked polyubiquitin chains

We conducted *in vitro* ubiquitination assays with recombinant proteins to identify E2(s) that cooperate with RNF213. As E3, we purified recombinant wild-type (WT) RNF213 RING domain with N-terminal GST and C-terminal HA fusion tags (GST-RNF213RING-WT). As an E3-dead negative control, we used GST-RNF213RING-C3997A (Fig. S1A in Supplementary Materials). Using Ubc13/Uev1A as E2, GST-RNF213RING-WT showed a pronounced induction of polyubiquitination in comparison with GST-RNF213RING-C3997A, demonstrating the functional coupling of RNF213 RING domain with this E2 (Fig. 1A). However, none of the other eleven

E2s tested; E2-25K, Ube2G2, UbcH2, UbcH3, UbcH4, UbcH5A, UbcH5B, UbcH6, UbcH7, UbcH8, or UbcH10, induced polyubiquitination with GST-RNF213RING-WT (Fig. 1B and Fig. S1B), although some did show autoubiquitination in the absence of E3. This suggests that the RNF213 RING domain exerts substantial E2 selectivity for its E3 activity. Next, to characterize the polyubiquitin chain linkages generated by RNF213 with Ubc13/Uev1A, we used a series of Ub mutants in which six of seven lysine residues are converted to arginines with the remaining lysine left intact, or all lysine residues are converted to arginines (K0-Ub). RNF213-catalyzed ubiquitination only occurred with K63-Ub, to a similar extent as WT Ub (Fig. 1C). In addition, K63-linkage-specific, but not K48-linkage-specific, anti-polyubiquitin antibodies reacted to polyubiquitin chains generated by RNF213 (Fig. 1D). Furthermore, these polyubiquitin chains could be deubiquitinated by AMSH (associated molecule with the SH3 domain of STAM), a K63-linkage-specific deubiquitinase (Fig. 1E). These results demonstrate that the RNF213 RING domain catalyzes K63-linked polyubiquitination using Ubc13/Uev1A.

3.2. Most RNF213 RING domain mutants are deficient in E3 activity

To date, nine mutations in the RNF213 RING domain of MMD patients have been reported [3,4]. To analyze the effects of these mutations on E3 activity, we purified GST-RNF213RING proteins harboring the C3997Y, P4007R, D4013N, H4014N, C4017S, R4019C,

W4024R, C4032R, or P4033L patient mutations (Fig. 2A). Examination of the E3 activities using Ubc13/Uev1A demonstrated that all RING domain mutants were polyubiquitination deficient, except for D4013N with an activity similar to WT, and for R4019C and W4024R with minimal but still discernible activities (Fig. 2B). To examine the structural consequences of these mutations, we constructed a 3D model of the RNF213 RING domain (dimer model) bound with Ubc13. Although RNF213 RING domain modeling was previously reported [4], this was based on the RING domain of RNF146 bound to UbcH5A which, from our *in vitro* ubiquitination assay (Fig. 1B), does not cooperate with RNF213. Therefore, we used the RNF8-Ubc13 complex [22] as template (Fig. 2C, D, and S2). Based on predictions, Cys-3997, His-4014, Cys-4017, and Cys-4032 are crucial amino acids that coordinate zinc ions to maintain the RING domain structure and enzymatic functions (Fig. 2D and S2A). Pro-4007 and Pro-4033, which are well-conserved in many RING domain-containing proteins, may affect protein stability and conformation of Cys-4032 and thus zinc coordination, respectively. Similarly, the R4019C mutation could affect zinc binding to Cys-4017 or Cys-4020 because of its proximity (Fig. 2D and S2B), whereas W4024R may affect Ubc13 binding (Fig. S2C). D4013N, located at the dimeric interface of RNF213 RING, may affect dimerization (Fig. S2D) although it did not impair E3 activity in our assays (Fig. 2B).

3.3. E3-deficient MMD patient mutations enhance NFκB activation and apoptosis in an AAA+ domain-dependent manner

Ubc13/Uev1A-mediated K63-linked polyubiquitination regulates various cellular events, including NFκB activation, DNA repair,

and endosomal transport [13]. Particularly, in the activation of the NFκB pathway, TNF receptor-associated factor 6 (TRAF6), a RING-type E3, generates K63-linked polyubiquitin chains with Ubc13/Uev1A, and these chains act as a scaffold to activate inhibitory κB (IκB) kinase [13]. More recently, RNF213 knockdown was shown to suppress palmitate-induced NFκB activation and apoptosis [9]. We therefore postulated that RNF213 could activate the NFκB pathway by generating K63-linked polyubiquitin chains similar to TRAF6. To test this possibility, we performed luciferase assays with an NFκB reporter plasmid, and found that full-length WT RNF213 overexpression indeed enhanced NFκB reporter activity in HEK293T cells (Fig. 3A), confirming that RNF213 positively regulates NFκB activation. Unexpectedly, however, as with the artificial E3-dead C3997A mutant, E3-deficient RNF213 mutants (C3997Y, P4007R, H4014N, C4017S, C4032R, and P4033L) showed enhanced, rather than impaired, NFκB activation in comparison with WT RNF213, although the effect of P4033L was mild (Fig. 3A). The D4013N mutation with unaffected E3 activity, and the R4019C and W4024R mutations with discernible E3 activities (Fig. 2B), activated NFκB similar to WT RNF213. The enhanced NFκB activation was not attributable to increased levels of mutant RNF213 proteins, which were in fact lower than that of WT (Fig. 3B). Indeed, examination of protein stabilities with CHX chase assays demonstrated that RNF213 mutants with high NFκB-inducing activity had shorter half-lives and significantly lower amounts of proteins remaining after 9 h of CHX treatment (Fig. 3C, D and S3). Interestingly, critical point mutations in both the Walker A and B of the first and second AAA+ domains (mAAA) [10], or deletion of the first AAA+ domain (dAAA), completely abrogated NFκB activation by RNF213 C3997Y or H4014N, respectively, indicating that the AAA+ domain is

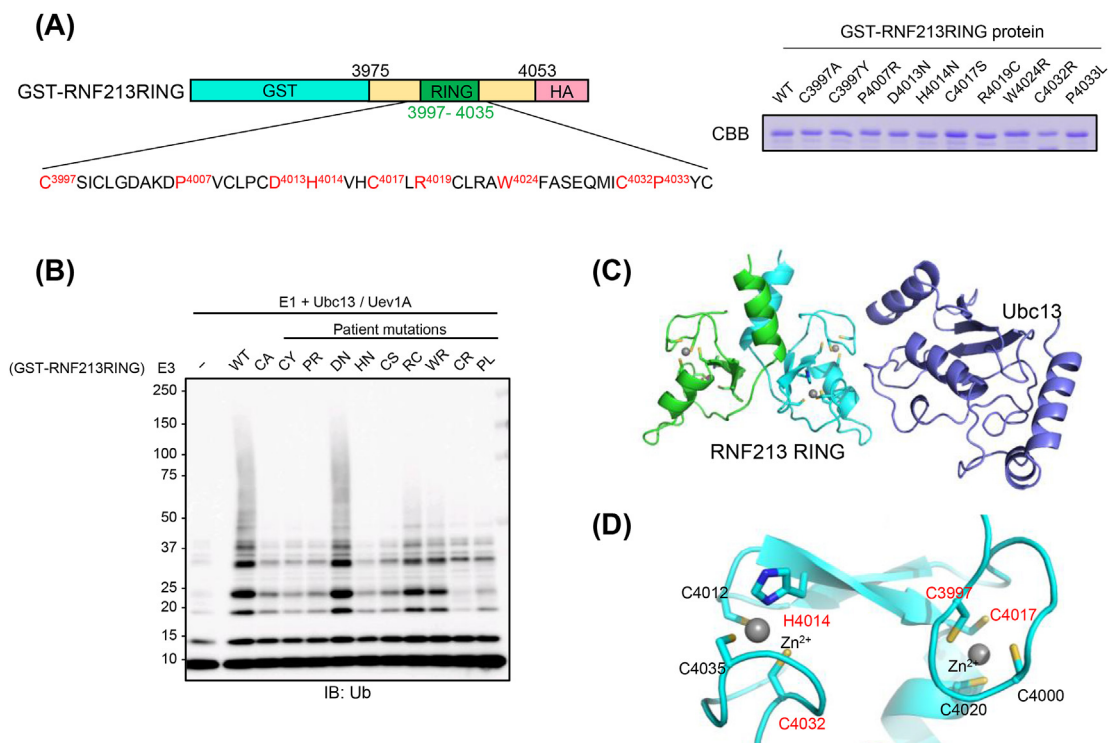


Fig. 2. Most RNF213 RING domain patient mutants are deficient in E3 activity.

(A) (left) Schematic diagram of GST-RNF213RING and MMD mutations, with positions shown in red. (right) Recombinant GST-RNF213RING proteins confirmed by CBB staining. (B) *In vitro* ubiquitination reaction performed using E1, E2 (Ubc13/Uev1A), and E3 (GST-RNF213RING, WT and various mutants), and probed with anti-Ub. (C) 3D structural model for RNF213 RING domain (green/cyan) bound to Ubc13 (light blue). Side chains that coordinate to Zn²⁺ ions (gray spheres) are shown as stick models. (D) Close-up view of Zn²⁺ binding sites of RNF213 RING showing localization of C3997, C4017, H4014 and C4032 residues. (For interpretation of the references to colour in this figure legend, the reader is referred to the Web version of this article.)

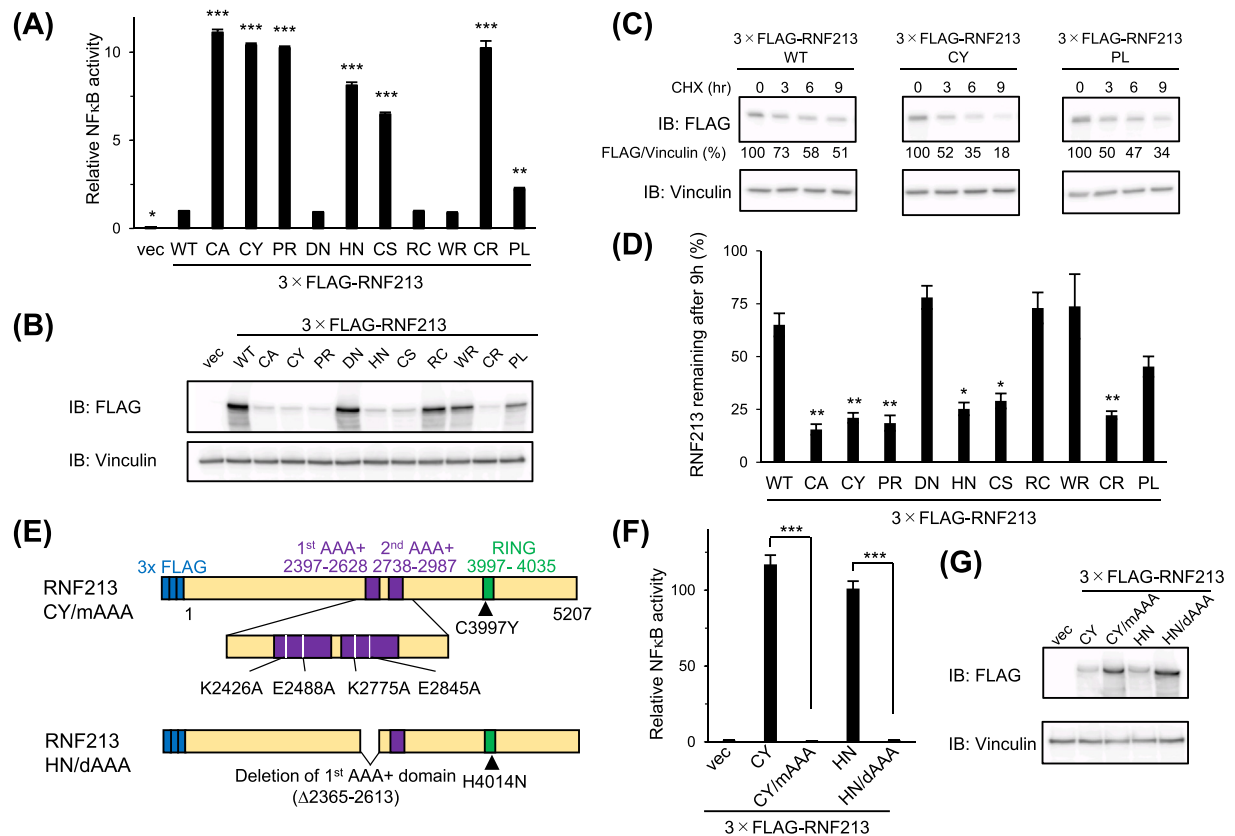


Fig. 3. E3-deficient MMD patient mutations greatly enhance NFκB activation.

(A) HEK293T cells transfected with firefly and Renilla luciferase constructs together with full-length 3xFLAG-RNF213 (WT or mutants) or pcDNA3.1 vector (vec). Data are normalized to Renilla luciferase and shown as mean \pm SEM (N = 3). Relative NFκB activity with WT RNF213 is defined as 1. (B) Cell lysates in (A) probed with anti-FLAG and anti-Vinculin. (C) HEK293T cells transfected with indicated 3xFLAG-RNF213 plasmids, treated with cycloheximide (CHX), and cell lysates at indicated time points probed with anti-FLAG and anti-Vinculin. 3xFLAG-RNF213 levels were normalized by Vinculin and relative protein levels at time 0 defined as 100. (D) RNF213 (WT and mutants) protein amounts remaining after 9 h of CHX treatment (N = 4, shown in Fig. S3). (E) Schematic diagram of RNF213 AAA+ domain mutants. (F) NFκB-reporter luciferase assays performed as in (A). Relative NFκB activity in cells with pcDNA3.1 defined as 1. ***p < 0.001. (G) Cell lysates used for luciferase assays in (F) probed with anti-FLAG and anti-Vinculin. (A, D) *p < 0.05, **p < 0.01, ***p < 0.001, vs WT 3xFLAG-RNF213.

essential for RNF213-induced NFκB activation (Fig. 3E and F). Furthermore, the RNF213 protein levels could be recovered by these AAA+ mutations (Fig. 3G).

As RNF213 has also been implicated in palmitate-induced apoptosis [9], we examined the effect of RNF213 MMD mutations on apoptosis by flowcytometric analysis with Annexin V and PI. Although WT RNF213 overexpression did not induce apoptosis in HEK293T cells, RNF213 mutants with high NFκB-inducing activity promoted both early (Annexin V+/PI-) and late (Annexin V+/PI+) apoptosis (Fig. 4A and S4). Furthermore, cleaved Caspase-3 was detected in lysates of cells overexpressing C3997Y or H4014N but not WT RNF213 (Fig. 4B), suggesting that Caspase-3 is activated by these RNF213 mutants. The D4013N, R4019C, and W4024R mutations that did not enhance NFκB activation also failed to induce apoptosis, indicating a positive correlation between NFκB- and apoptosis-inducing activities. In addition, AAA+ domain mutations greatly suppressed apoptosis induced by C3997Y or H4014N (Fig. 4C and S5), suggesting that both the NFκB- and apoptosis-inducing activities of RNF213 are dependent on the AAA+ domain. As the NFκB pathways can either positively or negatively regulate apoptosis, depending on cell types, conditions, or stimuli [23,24], we examined whether NFκB activation induced by RNF213 mutations could regulate apoptosis. Treatment of cells with QNZ, an inhibitor of NFκB activation [24], resulted in partial but significant

suppression of both NFκB activation and early apoptosis in C3997Y or H4014N overexpressing cells (Fig. 4D and S6). Although late apoptosis was unaffected by QNZ, this may be because QNZ was added 20 h post-transfection, by which time cell death may have already started and could not be prevented. Overall, these results suggest that mutant RNF213-induced NFκB activation positively regulates apoptosis in HEK293T cells.

4. Discussion

In this study, we identified Ubc13/Uev1A as an E2 enzyme that cooperates with the RNF213 RING domain to promote K63-linked polyubiquitination. Most MMD mutations in this domain greatly impaired the E3 activity, with the E3-deficient mutants particularly enhancing NFκB activation and apoptotic cell death in an AAA+ domain-dependent manner. These results suggest that the E3 activity of RNF213 may negatively regulate activation of NFκB and apoptosis, and that disruption of this regulation may be related to MMD pathogenesis.

Most RING-type E3 proteins that couple with Ubc13/Uev1A, including Cbl and RNF8, also use other E2s [21,25]. Although we tested 13 E2s in this study, there are ~40 E2s in humans [12] and it is therefore conceivable that other E2s also function with RNF213. While our results clearly demonstrate that RNF213 with Ubc13/

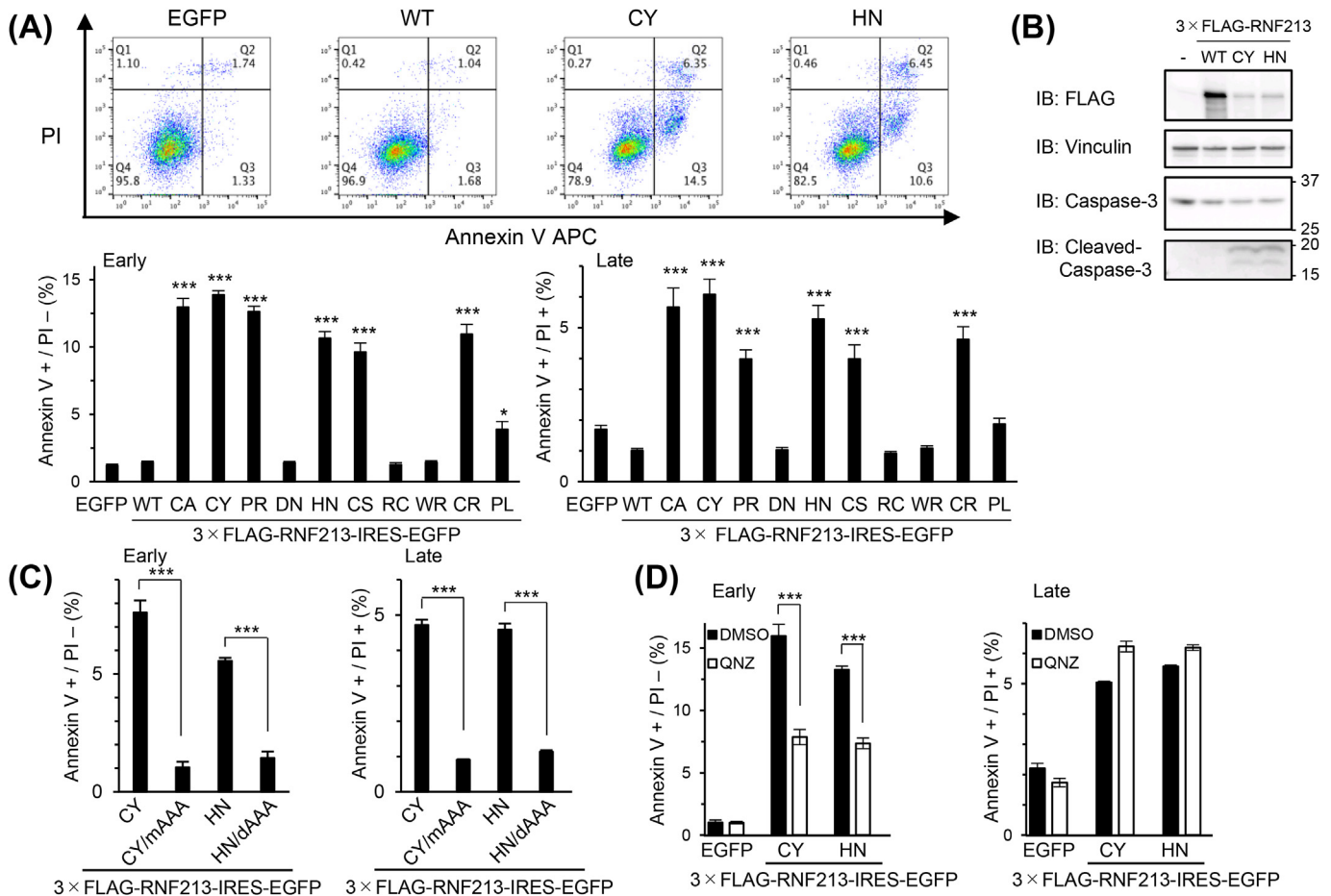


Fig. 4. E3-deficient MMD patient mutations induce apoptosis in HEK293 T cells.

(A) HEK293T cells transfected with the indicated expression plasmids, stained with Annexin V and propidium iodide (PI), and analyzed by flow cytometry gated on EGFP. Percentages of Annexin V⁺/PI⁻ (left) and Annexin V⁺/PI⁺ (right), representing early apoptotic and late apoptotic cells, respectively, are plotted (N = 5). Data represent mean ± SEM. *p < 0.05, ***p < 0.001, vs WT 3 × FLAG-RNF213. (B) Cell lysates probed with antibodies against FLAG, Vinculin, Caspase-3, and cleaved Caspase-3. (C) HEK293T cells transfected with indicated expression plasmids and analyzed as in (A) (N = 3). ***p < 0.001. (D) HEK293T cells transfected with the indicated expression plasmids with or without QNZ treatment, and analyzed as in (A) (N = 3). ***p < 0.001.

Uev1A form K63-linked polyubiquitin chains, and thereby effect specific intracellular processes, it is essential to identify bona fide RNF213 substrates, and clarify the effects of their RNF213-dependent polyubiquitination, to resolve the precise regulatory mechanisms of its E3 activity.

All RNF213 RING mutants that were deficient in E3 activity showed high NFκB activity and induced apoptosis when overexpressed in HEK293T cells, whereas the D4013N, R4019C and W4024R mutations, with normal or discernible E3 activities, showed NFκB and apoptotic levels comparable to WT RNF213. One possible reason why the latter three mutations did not evoke such increased activities may be related to the low penetrance of MMD; indeed there are reports of MMD unaffected D4013N or R4019C carriers within families [4,26]. Nevertheless, D4013N or R4019C overexpression in HUVEC have been shown to affect *in vitro* cell migration [16], indicating that the RNF213 mutation effects could be cell type-dependent. Further studies are clearly necessary to explain such allelic heterogeneity of RNF213 variants.

Our observation that RNF213 mutant proteins, with high NFκB and apoptotic activities, were unstable, raises the possibility that RNF213 protein stabilities are regulated by the NFκB or apoptotic pathways. Indeed, in NFκB activation, IκBα is phosphorylated by IκB kinase and subsequently degraded by the proteasome [13], while various substrates are processed by activated caspases during

apoptosis [27]. Whether such mechanisms are relevant to RNF213 protein stability, and the consequences of these processes on RNF213-regulated signaling events, must be clarified if the role of these mutations in MMD is to be resolved.

Several previous studies have suggested a relationship between MMD and NFκB activation or apoptosis. For example, an *in silico* analysis of genes co-expressed with RNF213 implied an association between RNF213 and NFκB pathways [28]. Furthermore, a clinical study suggested that the middle cerebral arteries of MMD patients have higher levels of cleaved Caspase-3 than controls [29], and that down-regulation of Cav-1, as observed in MMD patients, enhances apoptosis accompanied by Caspase-3 cleavage [30]. In addition, many patients with Majewski osteodysplastic primordial dwarfism type II, a severe condition highly susceptibility to apoptosis, also develop MMD [31]. Although the mechanisms and pathological significance of NFκB activation and apoptosis in such RNF213-related vasculopathies are unknown, it is tempting to speculate that mutation-induced apoptosis observed in our experiments can be extrapolated to vascular endothelial cells that are known to undergo dysfunction and possible apoptosis during MMD onset [3].

Finally, although our results clearly demonstrate that the AAA⁺ domain of RNF213, which regulates RNF213 oligomerization [10], is critical for NFκB activation and apoptosis, its precise role in these processes remains unknown. Further studies to clarify the

mechanisms of RNF213-mediated activation of NF κ B and apoptotic pathways, the interactions between the AAA⁺ and RING domains and their relevance to RNF213-related vasculopathies, are critical for understanding the pathogenesis of these diseases and for identifying potential targets for drug development.

Funding

This work was supported by Grant-in-Aid for Scientific Research on Innovative Areas (17H06397); JSPS-KAKENHI (17K08786); Astellas Foundation for Research on Metabolic Disorders; the Hakubi Project grant; and ISHIZUE 2019 of Kyoto University Research Development Program.

Declaration of competing interest

Dr. Akio Koizumi has a patent for RNF213 (P130009545), which does not alter adherence to all BBRC policies on sharing data and materials. Other authors declare no conflicts of interest.

Acknowledgements

We are grateful to Iara Barros for initiating the *in vitro* ubiquitination experiments, and to Dr. Akira Nishide and Dr. Yohei Mineharu for technical advice and helpful suggestions.

Appendix A. Supplementary data

Supplementary data to this article can be found online at <https://doi.org/10.1016/j.bbrc.2020.02.024>.

References

- [1] W. Liu, D. Morito, S. Takashima, et al., Identification of *RNF213* as a susceptibility gene for moyamoya disease and its possible role in vascular development, *PLoS One* 6 (2011), e22542, <https://doi.org/10.1371/journal.pone.0022542>.
- [2] F. Kamada, Y. Aoki, A. Narisawa, et al., A genome-wide association study identifies *RNF213* as the first Moyamoya disease gene, *J. Hum. Genet.* 56 (2011) 34–40, <https://doi.org/10.1038/jhg.2010.132>.
- [3] A. Koizumi, H. Kobayashi, T. Hitomi, et al., A new horizon of moyamoya disease and associated health risks explored through RNF213, *Environ. Health Prev. Med.* 21 (2016) 55–70, <https://doi.org/10.1007/s12199-015-0498-7>.
- [4] S. Guey, M. Kraemer, D. Herve, et al., Rare *RNF213* variants in the C-terminal region encompassing the RING-finger domain are associated with moyamoya angiopathy in Caucasians, *Eur. J. Hum. Genet.* 25 (2017) 995–1003, <https://doi.org/10.1038/ejhg.2017.92>.
- [5] H. Kobayashi, R. Kabata, H. Kinoshita, et al., Rare variants in *RNF213*, a susceptibility gene for moyamoya disease, are found in patients with pulmonary hypertension and aggravate hypoxia-induced pulmonary hypertension in mice, *Pulm. Circ.* 8 (2018), <https://doi.org/10.1177/2045894018778155>, 2045894018778155.
- [6] S. Okazaki, T. Morimoto, Y. Kamatani, et al., Moyamoya disease susceptibility variant *RNF213* p.R4810K increases the risk of ischemic stroke attributable to large-artery atherosclerosis, *Circulation* 139 (2019) 295–298, <https://doi.org/10.1161/CIRCULATIONAHA.118.038439>.
- [7] T. Hitomi, T. Habu, H. Kobayashi, et al., The moyamoya disease susceptibility variant *RNF213* R4810K (rs112735431) induces genomic instability by mitotic abnormality, *Biochem. Biophys. Res. Commun.* 439 (2013) 419–426, <https://doi.org/10.1016/j.bbrc.2013.08.067>.
- [8] M. Sugihara, D. Morito, S. Ainuki, et al., The AAA⁺ ATPase/ubiquitin ligase mysterin stabilizes cytoplasmic lipid droplets, *J. Cell Biol.* 218 (2019) 949–960, <https://doi.org/10.1083/jcb.201712120>.
- [9] M. Piccolis, L.M. Bond, M. Kampmann, et al., Probing the global cellular responses to lipotoxicity caused by saturated fatty acids, *Mol. Cell.* 74 (2019) 32–44, <https://doi.org/10.1016/j.molcel.2019.01.036>, e38.
- [10] D. Morito, K. Nishikawa, J. Hoseki, et al., Moyamoya disease-associated protein mysterin/RNF213 is a novel AAA⁺ ATPase, which dynamically changes its oligomeric state, *Sci. Rep.* 4 (2014) 4442, <https://doi.org/10.1038/srep04442>.
- [11] D. Komander, M. Rape, The Ubiquitin code, *Annu. Rev. Biochem.* 81 (2012) 203–229, <https://doi.org/10.1146/annurev-biochem-060310-170328>.
- [12] M.D. Stewart, T. Ritterhoff, R.E. Kleivit, et al., E2 enzymes: more than just middle men, *Cell Res.* 26 (2016) 423–440, <https://doi.org/10.1038/cr.2016.35>.
- [13] C.D. Hodge, L. Spyropoulos, J.N. Glover, Ubc13: the Lys63 ubiquitin chain building machine, *Oncotarget* 7 (2016) 64471–64504, <https://doi.org/10.18632/oncotarget.10948>.
- [14] M. Kim, T. Tezuka, K. Tanaka, et al., Cbl-c suppresses v-Src-induced transformation through ubiquitin-dependent protein degradation, *Oncogene* 23 (2004) 1645–1655, <https://doi.org/10.1038/sj.onc.1207298>.
- [15] R. Otsubo, M. Kim, J. Lee, et al., Midori-ishi Cyan/monomeric Kusabira-Orange-based fluorescence resonance energy transfer assay for characterization of various E3 ligases, *Gene Cell.* 21 (2016) 608–623, <https://doi.org/10.1111/gtc.12369>.
- [16] H. Kobayashi, M. Brozman, K. Kyselova, et al., *RNF213* rare variants in slovakian and Czech moyamoya disease patients, *PLoS One* 11 (2016), e0164759, <https://doi.org/10.1371/journal.pone.0164759>.
- [17] D. Morimoto, S. Isogai, T. Tenno, et al., Purification, crystallization and preliminary crystallographic studies of Lys48-linked polyubiquitin chains, *Acta Crystallogr. Sect. F Struct. Biol. Cryst. Commun.* 66 (2010) 834–837, <https://doi.org/10.1107/S1744309110018804>.
- [18] Y. Sato, A. Yoshikawa, A. Yamagata, et al., Structural basis for specific cleavage of Lys 63-linked polyubiquitin chains, *Nature* 455 (2008) 358–362, <https://doi.org/10.1038/nature07254>.
- [19] J. Choi, H. Kobayashi, H. Okuda, et al., β -cell-specific overexpression of adiponectin receptor 1 does not improve diabetes mellitus in Akita mice, *PLoS One* 13 (2018), e0190863, <https://doi.org/10.1371/journal.pone.0190863>.
- [20] M. Biasini, S. Bienert, A. Waterhouse, et al., SWISS-MODEL: modelling protein tertiary and quaternary structure using evolutionary information, *Nucleic Acids Res.* 42 (2014) W252–W258, <https://doi.org/10.1093/nar/gku340>.
- [21] M.S. Liyasova, K. Ma, D. Voeller, et al., Cbl interacts with multiple E2s *in vitro* and in cells, *PLoS One* 14 (2019), e0216967, <https://doi.org/10.1371/journal.pone.0216967>.
- [22] S.J. Campbell, R.A. Edwards, C.C. Leung, et al., Molecular insights into the function of RING finger (RNF)-containing proteins hRNF8 and hRNF168 in Ubc13/Mms2-dependent ubiquitylation, *J. Biol. Chem.* 287 (2012) 23900–23910, <https://doi.org/10.1074/jbc.M112.359653>.
- [23] S.K. Radhakrishnan, S. Kamalakaran, Pro-apoptotic role of NF- κ B: implications for cancer therapy, *Biochim. Biophys. Acta* 1766 (2006) 53–62, <https://doi.org/10.1016/j.bbcan.2006.02.001>.
- [24] X. Zhu, L. Huang, J. Gong, et al., NF- κ B pathway link with ER stress-induced autophagy and apoptosis in cervical tumor cells, *Cell Death Dis.* 3 (2017) 17059, <https://doi.org/10.1038/cddiscovery.2017.59>.
- [25] A. Paul, B. Wang, RNF8- and Ube2S-dependent ubiquitin lysine 11-linkage modification in response to DNA damage, *Mol. Cell.* 66 (2017) 458–472, <https://doi.org/10.1016/j.molcel.2017.04.013>, e455.
- [26] A.C. Cecchi, D. Guo, Z. Ren, et al., *RNF213* rare variants in an ethnically diverse population with Moyamoya disease, *Stroke* 45 (2014) 3200–3207, <https://doi.org/10.1161/STROKEAHA.114.006244>.
- [27] G.M. Cohen, Caspases: the executioners of apoptosis, *Biochem. J.* 326 (1997) 1–16, <https://doi.org/10.1042/bj3260001>.
- [28] K. Ohkubo, Y. Sakai, H. Inoue, et al., Moyamoya disease susceptibility gene *RNF213* links inflammatory and angiogenic signals in endothelial cells, *Sci. Rep.* 5 (2015) 13191, <https://doi.org/10.1038/srep13191>.
- [29] Y. Takagi, K. Kikuta, N. Sadamasa, et al., Caspase-3-dependent apoptosis in middle cerebral arteries in patients with moyamoya disease, *Neurosurgery* 59 (2006) 894–900, <https://doi.org/10.1227/01.NEU.0000232771.80339.15>.
- [30] J.W. Chung, D.H. Kim, M.J. Oh, et al., Cav-1 (Caveolin-1) and arterial remodeling in adult moyamoya disease, *Stroke* 49 (2018) 2597–2604, <https://doi.org/10.1161/STROKEAHA.118.021888>.
- [31] A. Rauch, C.T. Thiel, D. Schindler, et al., Mutations in the pericentriar (*PCNT*) gene cause primordial dwarfism, *Science* 319 (2008) 816–819, <https://doi.org/10.1126/science.1151174>.